HHS Public Access

Author manuscript

Mol Cell Endocrinol. Author manuscript; available in PMC 2018 February 05.

Published in final edited form as:

Mol Cell Endocrinol. 2017 February 05; 441: 124–133. doi:10.1016/j.mce.2016.10.014.

Immunohistochemistry of aldosterone synthase leads the way to the pathogenesis of primary aldosteronism

Koshiro Nishimoto[a,c,*,1], **Minae Koga**[f,1], **Tsugio Seki**[g], **Kenji Oki**[h], **Elise P. Gomez-Sanchez**[i], **Celso E. Gomez-Sanchez**[j], **Mitsuhide Naruse**[k], **Tomokazu Sakaguchi**[l], **Shinya Morita**[d], **Takeo Kosaka**[d], **Mototsugu Oya**[d], **Tadashi Ogishima**[m], **Masanori Yasuda**[b], **Makoto Suematsu**[c], **Yasuaki Kabe**[c], **Masao Omura**[f], **Tetsuo Nishikawa**[f], and **Kuniaki Mukai**[c,e,**]

[a]Department of Uro-Oncology, Saitama Medical University International Medical Center, Hidaka 350-1241, Japan

[b]Department of Pathology, Saitama Medical University International Medical Center, Hidaka 350-1241, Japan

[c]Department of Biochemistry, Keio University School of Medicine, 35 Shinanomachi, Shinjuku-ku, Tokyo 160-8582, Japan

[d]Department of Urology, Keio University School of Medicine, 35 Shinanomachi, Shinjuku-ku, Tokyo 160-8582, Japan

[e]Department of Medical Education Center, Keio University School of Medicine, 35 Shinanomachi, Shinjuku-ku, Tokyo 160-8582, Japan

[f]Endocrinology & Diabetes Center, Yokohama Rosai Hospital, Yokohama 222-0036, Japan

[g]Department of Medical Education, School of Medicine, California University of Science and Medicine, 1405 West Valley Blvd #101, Colton, CA 92324, USA

[h]Department of Molecular and Internal Medicine, Graduate School of Biomedical and Health Sciences, Hiroshima University, Hiroshima 734-8551, Japan

[i]Department of Pharmacology & Toxicology, University of Mississippi Medical Center, Jackson, MS 39216, USA

[j]Endocrinology Section, G.V. (Sonny) Montgomery VA Medical Center and University of Mississippi Medical Center, Jackson, MS 39216, USA

[k]Department of Endocrinology, Metabolism and Hypertension, Clinical Research Institute, National Hospital Organization Kyoto Medical Center, Kyoto 612-8555, Japan

[l]Department of Surgery, Misato Kenwa Hospital, 4-494-1 Takano, Misato, Saitama 341-8555, Japan

[m]Department of Chemistry, Faculty of Sciences, Kyushu University, Fukuoka 819-0395, Japan

[*]Corresponding author. Department of Uro-Oncology, Saitama Medical University International Medical Center, Hidaka 350-1241, Japan. [**]Corresponding author. Department of Medical Education Center, Keio University School of Medicine, 35 Shinanomachi, Shinjuku-ku, Tokyo 160-8582, Japan.

[1]Co-first authors.

Abstract

Our group previously purified human and rat aldosterone synthase (CYP11B2 and Cyp11b2, respectively) from their adrenals and verified that it is distinct from steroid 11β-hydroxylase (CYP11B1 or Cyp11b1), the cortisol- or corticosterone-synthesizing enzyme. We now describe their distributions immunohistochemically with specific antibodies. In rats, there is layered functional zonation with the Cyp11b2-positive zona glomerulosa (ZG), Cyp11b1-positive zona fasciculata (ZF), and Cyp11b2/Cyp11b1-negative undifferentiated zone between the ZG and ZF. In human infants and children (<12 years old), the functional zonation is similar to that in rats. In adults, the adrenal cortex remodels and subcapsular aldosterone-producing cell clusters (APCCs) replace the continuous ZG layer. We recently reported possible APCC-to-APA transitional lesions (pAATLs) in 2 cases of unilateral multiple adrenocortical micronodules. In this review, we present 4 additional cases of primary aldosteronism, from which the extracted adrenals contain pAATLs, with results of next generation sequencing for these lesions. Immunohistochemistry for CYP11B2 and CYP11B1 has become an important tool for the diagnosis of and research on adrenocortical pathological conditions and suggests that APCCs may be the origin of aldosterone-producing adenoma.

Keywords

Aldosterone synthase (CYP11B2); Immunohistochemistry; Rat adrenal; Human adrenal; Aldosterone-producing cell cluster (APCC); Possible APCC-to-APA transitional lesion (pAATL)

1. Introduction: aldosterone production from physiology to pathophysiology

1.1. Physiological layered structure of the adrenal cortex (functional zonation)

Aldosterone is synthesized in the zona glomerulosa (ZG), the outermost zone of the adrenal cortex in rats and humans. The renin-angiotensin system primarily regulates the plasma level of aldosterone by inducing several factors including the aldosterone synthase (CYP11B2). Glucocorticoids (cortisol and corticosterone) are produced in the zona fasciculata (ZF), the mid zone, and adrenal androgens are formed in the zona reticularis (ZR), the innermost zone. The classical observation that the different zones produce distinct steroid hormones is referred to as ‘functional zonation’ in the adrenal cortex.

1.2. Pathological aldosterone production in humans

Dysregulation of aldosterone synthesis resulting in excessive aldosterone production despite suppressed renin and angiotensin is known as primary aldosteronism (PA). PA is the most common cause of endocrine hypertension and of secondary hypertension (Funder et al., 2008; Nishikawa et al., 2011). One or both adrenals may be affected; aldosterone-producing adenomas (APAs) are responsible for most unilateral PA. In the past several years, somatic mutations in a subset of ion channel and pump genes have been reported in APAs (APA-associated mutations) (Azizan et al., 2013; Beuschlein et al., 2013; Scholl et al., 2013; Choi et al., 2011) and the prevalence of each mutation in APAs has been reported in a large scale cohort study (Boulkroun et al., 2012). These diverse mutations directly or indirectly increase

intracellular calcium concentrations leading to increased expression and activity of the CYP11B2 enzyme and excessive aldosterone production, however their effect on cell proliferation in *in vitro* systems has been variable, calling into question the role of these mutations in adenoma formation (Azizan et al., 2013; Beuschlein et al., 2013; Scholl et al., 2013; Choi et al., 2011; Gomez-Sanchez and Gomez-Sanchez, 2012; Akerstrom et al., 2012; Oki et al., 2012).

1.3. Novel findings on the human adrenal cortex by immunohistochemistry

Until several years ago, functional zonation in humans, including aldosterone production, had not been visualized due to the absence of effective methods for immunohistochemistry that distinguished between CYP11B1 and CYP11B2. Antigen-activation for immunohistochemistry with our in-house antibodies, which had been developed against the two enzymes (Ogishima et al., 1991) (see Section 2.2), provided the first distinct images of functional zonation under normal and pathological conditions including APA (Nishimoto et al., 2010) and demonstrated for the first time aldosterone-producing cell clusters (APCCs) (see Section 4). APCCs may be a link between the physiology and pathophysiology of aldosterone production.

2. Identity of the enzyme catalyzing the final step of aldosterone synthesis in rats and humans

2.1. Rats

In the mid 1980s, it was suggested that rats have two separate enzymes for aldosterone and corticosterone syntheses. Upon increasing aldosterone production by the feeding a low salt diet, a novel enzyme distinct from the steroid 11β-hydroxylase described previously was found to be induced, both of which were recognized by an anti-bovine 11β-hydroxylase antibodies (Lauber et al., 1987; Ohnishi et al., 1988). Using high performance liquid chromatography (HPLC), our group purified two enzymes (molecular weights: 49.5 kDa and 51.5 kDa) from the rat adrenal capsular portion (i.e., adrenal capsule and ZG) and only the 51.5 kDa enzyme from the decapsulated portion (i.e., ZF, ZR, and medulla) (Ogishima et al., 1989). The 51.5 kDa protein exhibited 11β-hydroxylase and 18-hydroxylase activities, but not 18-oxidase activity, indicating that it was a corticosterone-producing enzyme, currently known as Cyp11b1. The 49.5 kDa enzyme was capable of catalyzing 11β-hydroxylation, 18-hydroxylation, and 18-oxidation, indicating that it was aldosterone synthase. We termed the 49.5 kDa protein P450aldo (Ogishima et al., 1989) and determined its cDNA and genomic DNA sequences (Mukai et al., 1993; Imai et al., 1990), currently known as Cyp11b2.

2.2. Humans

In humans, a pair of 11β-hydroxylase-related genes, *CYP11B1* and *CYP11B2*, was cloned in 1989 (Mornet et al., 1989), although expression of CYP11B2 gene was still unknown. The two genes had markedly high homology at the DNA (95% in coding regions and about 90% in introns) and amino acid (93%) levels. Using the same HPLC method (see Section 2.1), our group purified two proteins that were reactive to an anti-bovine 11β-hydroxylase antibody, and demonstrated that the 48.5 kDa protein isolated from APAs exhibited 18-

oxidase activity (i.e. aldosterone synthase, CYP11B2), whereas the 50 kDa protein did not (i.e. cortisol synthesizing enzyme, CYP11B1) (Ogishima et al., 1991). We generated a pair of specific antibodies against CYP11B1 and CYP11B2 using two similar but different peptides (RYNLGGPRMVC and RYDLGGAGMVC for CYP11B2 and CYP11B1, respectively) from their deduced amino acid sequences (Mornet et al., 1989), which successfully confirmed that the purified 48.5 kDa and 50 kDa proteins were in fact the CYP11B2 and CYP11B1 gene product by Western blot (Ogishima et al., 1991) (Data for CYP11B1 was shown later (Nishimoto et al., 2010)). Other research groups confirmed our results by producing recombinant CYP11B1 and CYP11B2 in cultured mammalian cells, and by demonstrating their enzymatic activities of 11β-hydroxylase and aldosterone synthase, respectively (Curnow et al., 1991; Kawamoto et al., 1992).

3. Spatial arrangement of CYP11B2 and CYP11B1 in rodents and human adrenal cortex

3.1. Rats and mice

In 1992, our group also generated a pair of antibodies with the ability to distinguish between rat Cyp11b2 and Cyp11b1 and revealed the distribution of the rat Cyp11b2 and Cyp11b1 in the ZG and ZF-ZR of rat adrenal glands, respectively, by immunohistochemistry (Ogishima et al., 1992). Double-immunostaining using these antibodies identified a layer negative for both Cyp11b2 and Cyp11b1 between the ZG and ZF, which we termed the undifferentiated zone (Mitani et al., 1994). The same pair of *Cyp11b* genes was cloned for the mouse and their distinct distributions were verified by *in situ* hybridization (Domalik et al., 1991). Monoclonal antibodies for the rat enzymes generated by our collaborator Dr. Gomez-Sanchez showed the same findings with the rat adrenals (Wotus et al., 1998; Nishimoto et al., 2014; Nishimoto et al., 2013; Nishimoto et al., 2012). Thus, the Cyp11b1 and Cyp11b2 are localized in a mutually exclusive manner in rats and mice consistent with the classical view of the layered functional zonation of adrenocortical hormonal production.

3.2. Humans

In contrast to the rodents, the histochemical localization of the two human enzymes was left unresolved after the identification of the enzymes and their genes because none of the antibodies against CYP11B family proteins functioned well in the immunohistochemical staining of human adrenal sections. Several attempts using *in situ* hybridization techniques were reported for *CYP11B2* and *CYP11B1*, but they did not clearly define their distributions, which may have been due to the low specificity of the analysis (Erdmann et al., 1995; Pascoe et al., 1995; Enberg et al., 2004; Shigematsu et al., 2006). Consequently, the spatial arrangement of the two human enzymes was not clarified until we attempted a new antigen-retrieval protocol on formalin-fixed paraffin-embedded (FFPE) human adrenal sections nearly two decades after the development of antibodies against the two enzymes (the antibodies described in Section 2.2) (Nishimoto et al., 2010).

4. Histology of human aldosterone production under normal and pathological conditions

4.1. Normal adult adrenal cortex

Immunohistochemical analyses of normal adrenals uncovered an unexpected expression pattern of CYP11B2 in some adult adrenal cortex samples (Nishimoto et al., 2010). In contrast to CYP11B2-positive cells sparsely, but relatively evenly distributed within the ZG, the novel pattern showed a cluster of CYP11B2-positive cells in subcapsular areas corresponding to the ZG and part of the ZF, which are separated from the surrounding CYP11B1-positive areas by a defined border. ZG and ZF cells are morphologically distinct. ZG cells are smaller with a smaller cytoplasm to nucleus ratio than the ZF cells with foamy-appearing cytoplasm due to many lipid droplets. The aldosterone producing cell-cluster, APCC, is characterized by strong, uniform immunoreactivity for CYP11B2 and no CYP11B1 in cells with ZG morphology and an inner columnar ZF-like cells forming cords. APCCs are 0. 2–1.5 mm range in width along the capsular length and 0.1–0.5 mm in depth at the farthest point perpendicular to the capsule. One or more APCCs are detectable in most normal adult adrenals. The ZG-type (layered) expression of CYP11B2 was seldom detected in sections with many APCCs, suggesting that normal aldosterone production in the ZG may be suppressed due to autonomous aldosterone production from APCCs.

4.2. Remodeling of the human adrenal cortex

Our group recently double-immunostained adrenal tissues prepared from autopsied patients aged between 0 and 50 years old for CYP11B2 and CYP11B1 (Nishimoto et al., 2016a). All adrenals from patients younger than 12 years old had a layered ZG and ZF without apparent APCCs. In this age group, some adrenals had an unstained (CYP11B2/CYP11B1-negative) layer between the ZG and ZF, resembling the rat undifferentiated zone (Mitani et al., 1994). In contrast, many adrenal samples from patients aged 18 years and older had APCCs. For the manuscript, four investigators independently measured the ratio of APCC areas over the whole adrenal area and number of APCCs and found that the averages of the two values increased with age. Thus, we currently hypothesize that the adrenal cortex with layered zonation in children remodels to develop APCCs in many adults over time.

4.3. CYP11B2 and CYP11B1 localization in adrenocortical hormone excess diseases

An immunohistochemical examination of adrenal tumors for CYP11B2 and CYP11B1 was shown to be useful for reaching confirmatory diagnoses of apparent APAs, aldosterone-producing micronodules, cortisol-producing adenomas (CPAs), and unclassified pathological conditions such as PA due to multiple APCCs (Nishimoto et al., 2010; Sakuma et al., 2014; Dekkers et al., 2014; Nanba et al., 2013). Immunohistochemistry for CYP11B2 and CYP11B1 is more reliable than that of 3β-hydroxysteroid dehydrogenase (3βHSD, an upstream enzyme for both CYP11B2 and CYP11B1) and 17α-hydroxylase/17, 20 lyase (CYP17, an upstream enzyme for CYP11B1, but not CYP11B2) (Sasano, 1994). Recently-developed monoclonal antibodies for CYP11B2 and CYP11B1 may play an important role in the development of adrenal pathological diagnostic and aldosterone-research fields (Gomez-Sanchez et al., 2014).

4.4. APA, CPA, and aldosterone-producing adrenocortical carcinoma (ACC)

In traditional hematoxylin and eosin (H&E) staining, APA and CPA comprise heterogeneous tumor cells and APAs are generally larger (>3 mm) than APCCs (<1.5 mm). Double-immunostaining revealed that APAs include CYP11B2- and CYP11B1-positive cells, while CPAs consist of CYP11B1-positive cells only. The expression of 3βHSD and CYP17 is coordinated for the intended hormone synthesis in APAs and CPAs; CYP11B2-positive cells are positive for 3βHSD, but not for CYP17, while CYP11B1-positive cells are positive for 3βHSD and CYP17. We previously reported that the coordinated expression of these enzymes was disorganized in aldosterone-producing ACC, which may be due to the extreme dysplasia of ACC cells (Uchida et al., 2016). In ACC, a large number of CYP11B2-positive cells are negative for 3βHSD, but enough are positive for 3βHSD to support high autonomous synthesis of aldosterone.

4.5. Pathological roles of APCCs

The presence of APCCs in the histologically normal adrenal region adjacent to an APA suggests that APCCs autonomously produce aldosterone even under low levels of renin and angiotensin II (see Case 3 in Section 5.4) (Nishimoto et al., 2010). Nishimoto, Tomlins, and Rainey et al. recently showed that APCCs have higher *CYP11B2* mRNA expression levels than the ZG, ZF, and ZR and that some APCCs carry APA-associated somatic mutations (Nishimoto et al., 2015). These findings led us to hypothesize that APCCs are the initial pathological structure that produces aldosterone autonomously and are the origin of APAs. Further molecular analyses, along with the development of *in vitro* and *in vivo* models of APCCs, are needed to test this hypothesis.

5. Possible APCC-to-APA transitional lesions (pAATLs)

5.1. pAATLs in unilateral multiple (adrenocortical micro-) nodules (UMNs)

We recently reported pAATLs (Nishimoto et al., 2016b) in 2 cases of UMNs that were previously described by our collaborators (Omura et al., 2002). These pAATLs consist of subcapsular APCC-like and inner micro-APA-like (mAPA-like) portions without an apparent histological border. The APCC-like portion histologically consists of ZG-like and inner ZF-like cells and is immunohistochemically positive for CYP11B2, but not CYP11B1. The mAPA-like portion consists of a heterogeneous mixture of CYP11B1-positive cells and CYP11B2-positive cells. We performed next generation sequencing (NGS) analyses using isolated DNA from pAATLs, detected APA-associated mutations in both portions, and concluded that the introduction of APA-associated mutations in the ion channel/pump genes may be involved in the development of mAPA from existing APCCs. In this review, we describe 4 additional cases of pAATLs below, which were diagnosed as unilateral PA according to the clinical practice guidelines for PA (Table 1) (Funder et al., 2008; Nishikawa et al., 2011) and underwent laparoscopic adrenalectomy (Sections 5.2–5.5).

5.2. Case 1

Case 1 was a 64 year-old male, who was referred to the Hiroshima University Hospital for evaluation of hypertension. He had normal appearance with normal body mass index (BMI:

21.9 kg/m^2 [normal range < 25 kg/m^2]). Blood tests showed high plasma aldosterone concentration (PAC: 214 pg/mL [39–159 pg/mL]) and normal plasma renin activity (PRA: 0.4 ng/ml/h [0.3–2.9 ng/ml/h]), thus high aldosterone/renin ratio (ARR, 535.0, [cut off < 200]), suggesting that he had PA (see also Table 1 for test results of all patients). ARR and % decrease of PAC after captopril loading were 485 (cut off < 200 (Nishikawa et al., 2011)) and 26.5% (cut off < 30% (Funder et al., 2008)), respectively (captopril challenge test). PRA after furosemide infusion with 2 h-upright stimulation was low (0.9 ng/mg/h (Nishikawa et al., 2011)). These two tests confirmed that he had PA. An adrenal venous sampling test suggested that the left adrenal produced more aldosterone than the right adrenal (lateralized ratio: 5.12 [cut off values of Japanese and US guidelines were 4 and 2.6, respectively]) (Funder et al., 2008; Nishikawa et al., 2011). The patient underwent laparoscopic left adrenalectomy and his hypertension was cured (post-operative PAC and PRA were 110 pg/mL and 1.0 ng/ml/hr, respectively).

The left adrenal from Case 1 was diagnosed as UMN, due to its histopathology of multiple small nodules/section (*in Fig. 1A). The immunohistochemical analysis (Fig. 1B) revealed that the small nodules resembled pAATLs of the cases described above (see Section 5.1) (Nishimoto et al., 2016a,b) with a subcapsular APCC-like portion (80 in Fig. 1B–D) and inner mAPA-like portion (81 in Fig. 1B–D). The largest pAATL (pAATL#9, 6 mm in length) had a limited area of APCC-like portion compared to other pAATLs (pAATL#8, #10, and #11). This suggests either that in this lesion the APCC-like portion resided outside of the section plane or that it had mostly transitioned to a mAPA. In order to clarify if the APCC-like portion and mAPA-like portion were continuous, we performed Sirius Red staining which labels collagen fibers on a serial section used for microdissection (Fig. 1E). No obvious fibrous border was found between the APCC-like and mAPA-like portions and the tissue was microscopically continuous between these portions. Thus, we concluded that the pAATL was a single continuous entity rather than an individual APCC and a micro-nodule.

5.3. Case 2

Case 2 was a 61 year-old male, who was referred to the Misato Kenwa Hospital for evaluation of hypertension. He had normal appearance with normal BMI (19.6 kg/m^2). Blood test showed high ARR (PAC [198 pg/mL]/PRA [0.3 ng/ml/h] = 660), suggesting that he was PA. ARR and % decrease of PAC after captopril loading were 189.6 and 40%, respectively (negative result). PRA after furosemide infusion with 2 h-upright stimulation was low (1.4 [cut off <2.0] ng/ml/h, furosemide upright test (Nishikawa et al., 2011)). Although the captopril challenge test was negative, the furosemide upright test led to a diagnosis of PA. In addition, computed tomography showed left adrenal hyperplasia. Then, he underwent adrenal venous sampling test. Based on plasma cortisol concentration (PCC) values, adrenal venous samples were adequately collected from both adrenal glands ([an adrenal PCC ≥ 200 μg/dL] and/or [an adrenal PCC ≥ 5 times higher than peripheral venous PCC] (Nishikawa et al., 2011) [Table 1]). PAC from left adrenal vein was extremely high (72,800 pg/mL, cut off >14,000 pg/mL) while that from right adrenal was not (9100 pg/mL), suggesting that the left adrenal contained an aldosterone-producing lesion(s) (Nishikawa et al., 2011). Further, lateralized ratio (7.5, cut off > 2.6) and contralateral ratio (0.7, cut off < 1) of the adrenal venous sampling test supported that the left adrenal produced more

aldosterone than right (Funder et al., 2008; Nishikawa et al., 2011). He underwent laparoscopic left adrenalectomy and his hypertension was cured.

The adrenal from Case 2 was diagnosed as a single hyperplastic nodule (* in Fig. 2A, 4.2 mm in length) between subcapsular normal adrenal cortex (** in Fig. 2A) and adrenal medulla (m in Fig. 2A). Immunohistochemically, the adrenal cortex adjacent to the nodular lesion was considered subcapsular APCC, because it consisted of groups of cells with ZG- and ZF-like morphology (** in Fig. 2A) and expressed CYP11B2, but not CYP11B1 (** in Fig. 2B). The nodular portion was like a mAPA as it comprised more than 90% compact cells with fewer than 10% clear cells irregularly intermingled (* in Fig. 2A). More than 95% of the cell expressed CYP11B2; fewer than 5% expressed CYP11B1 (arrows in Fig. 2B). The expression patterns of these enzymes were consistent with normal steroidogenic pathways: i.e., CYP11B2-positive cells expressed 3βHSD, but not CYP17, while CYP11B1-positive cells expressed 3βHSD and CYP17 (Fig. 2C and D) as reported recently (Nishimoto et al., 2010). Sirius Red staining identified a fibrous border between normal adrenal gland and the mAPA-like lesion (black arrows in Fig. 2E, the panel E corresponds to the boxed area in Fig. 2A). No obvious fibrous border was seen between the APCC-like portion and mAPA-like portion (red arrows in Fig. 2E). Thus, as in Case 1, we concluded that the pAATL in Case 2 is histologically continuous.

5.4. Case 3

A 35 year-old woman was referred to the Yokohama Rosai Hospital for evaluation and treatment of PA. Blood test showed high ARR (PAC [229 pg/mL]/PRA [0.4 ng/ml/h] = 572), suggesting that she had PA. A computed tomography revealed 9 mm and 7 mm tumors in the left adrenal. PAC after saline infusion was high (336 pg/mL, saline infusion test, cut off < 60 (Nishikawa et al., 2011)). ARR and % decrease of PAC after captopril loading were 283 and 8.7%, respectively. PRA after furosemide infusion with 2 h-upright stimulation was 0.8 ng/ml/h. These three tests confirmed the diagnosis of PA. Adrenal venous sampling suggested autonomous aldosterone production from left adrenal gland (lateralized ratio: 4.96, contralateral ratio: 0.84). She underwent laparoscopic left adrenalectomy and her PA was cured.

Two APAs were diagnosed by pathology (APA #1: #14 in Fig. 3A; APA #2 is not shown). Immunohistochemistry revealed that the APAs strongly expressed CYP11B2 (#14 in Fig. 3B) and the adjacent adrenal cortex contained a large number of APCCs (blue arrowheads in Fig. 3B). We detected an additional small (1.5 mm) nodule that may be another type of pAATL (C and D in Fig. 3A and B, respectively, which are enlarged in Fig. 3C and D). This pAATL was distinct from those in Cases 1–2, because it consisted of a mixture of CYP11B2-positive cells and CYP11B1-positive cells similar to APAs, had a columnar arrangement similar to APCCs, but was not subcapsular as expected for APCCs. This case was presented at the Adrenal Cortex 2016 meeting in Boston.

5.5. Case 4

Case 4 was a 37 year-old young male who suffered from severe headache due to malignant hypertension (systolic blood pressure > 220 mmHg) and was immediately hospitalized at the

National Hospital Organization Kyoto Medical Center. He had normal appearance with normal BMI (23.7 kg/m^2). Blood test showed high ARR (332), suggesting that he was PA. ARR and % decrease of PAC after captopril loading were 312.5 and 3.8%, respectively. Saline infusion did not suppress PAC (80 pg/mL). PRA after furosemide infusion with 2 h-upright stimulation was low (1.3 ng/ml/h). Although the saline infusion test was negative, results of the captopril challenge and furosemide upright test led to a diagnosis of PA. According to a proposed diagnostic criteria for subclinical Cushing's syndrome (Akehi et al., 2013), cortisol production was clinically normal: serum cortisol concentration [SCC] in the morning, at night, and after 1 mg dexamethasone suppression were 7.3 μg/dL (cut off < 23.9 μg/dL), 1.4 μg/dL (<5 μg/dL), and 1.4 μg/dL (<1.8 μg/dL), respectively. Adrenal venous sampling indicated that his PA was due to autonomous aldosterone production from left adrenal gland (lateralized ratio: 6.3, contralateral ratio: 0.6). Left adrenalectomy led to complete remission of PA, however within half a year his hypertension recurred.

The adrenal from Case 4 was diagnosed by histopathology as diffuse and nodular hyperplasia (Fig. 4A). Immunohistochemistry revealed that the adrenal had multiple CYP11B2-positive lesions (Fig. 4B). While the pAATLs in Cases 1–3 grew from the subcapsular area to the medulla by invading the ZF and ZR, the lesions in Case 4 appeared to grow outward by thickening of the subcapsular regions, leaving the ZF and ZR intact. These lesions possessed the characteristics of APCCs in the following two points (see Section 3.2): (i) they were comprised of cells express strong, uniform immunoreactivity for CYP11B2 but not for CYP11B1/CYP17 (Fig. 4B,D), (ii) some portions consisted of ZF-like cells forming cords (Fig. 4A). Although the lesions harbored APCC-like properties, we acknowledge that they might be closer to APAs in that the cells in these lesions looked like they had high proliferation activity (Fig. 4A). Thus, Case 4 might be a different type of possible APCC-to-APA transitional lesion, i.e., pAATL. Intriguingly, the multiple CYP11B2-positive areas had no APA-associated mutation (see Section 5.6). Further examination of similar cases are needed to conclude the nature of this type of lesion.

5.6. NGS analyses for cases 1, 3, and 4

We microdissected small amount of control tissues from ZF and ZR (Controls #5 [DNA #79 in Fig. 1B], #6 [DNA #15, not shown in Fig. 3], and #7 [DNA #17 in Fig. 4B] for Cases 1, 3, and 4, respectively; Table 2), pAATLs (pAATL #8–11, 13, as well as 16 and 18 for Cases 1, 3, and 4, respectively; Table 2), and APAs (APA #1 and 2 for Case 3). DNA and RNA were isolated from these tissues, and were used in quantitative real-time PCR analyses for *CYP11B2* (CYP11B2-qPCR) and NGS for reported APA-associated mutations, as previously described (Table 2, detailed sequence data are shown in Supplemental Tables 1 and 2) (Nishimoto et al., 2015, 2016a,b). For the NGS, we used a custom Ion Torrent AmpliSeq Panel (APA_v13) with 12 multiplexed amplicons targeting the 20 hot spot mutation sites of *ATP1A1*, *ATP2B3*, *CACNA1D*, and *KCNJ5* found in APA. The validity of this approach, i.e., the use of the custom panel on FFPE section tissues, was confirmed in our previous reports, where the mutations identified in FFPE samples were confirmed in the matching flash frozen tissues by Sanger sequencing (Nishimoto et al., 2016a,b; Tamura et al., 2016). However, also in the reports, we showed that the small amount of damaged DNA purified from FFPE sections was not sufficient or suitable for conventional Sanger

sequencing, and therefore, the Sanger sequencing was not performed in this report. We confirmed that all pAATL and APA samples had higher CYP11B2 expression levels than those of controls, indicating successful sampling (Table 2). Well documented *KCNJ5* mutations were detected in the largest pAATL in Case 1 (pAATL #9, Fig. 1B; DNA #82; p. Gly151Arg, Table 2) and in APAs in Case 3 (APA #1, DNA #14, Fig. 1A and B; APA #2, DNA #13, image is not shown; p.Leu168Arg, Table 2), suggesting that *KCNJ5* mutations frequently occur in larger aldosterone-producing lesions. Several sequence variants were detected in Case 1 pAATLs, however some of these may have been due to extended PCR amplifications (30 cycles, Table 2). The pAATL #13 in Case 3 also harbored mutations, although they were different from the *KCNJ5* mutations detected in both APA #1 and #2. The pAATLs in Case 4 did not harbor a mutation.

6. Conclusions and perspectives

Immunohistochemistry for CYP11B2 and CYP11B1 is a powerful tool for identifying aldosterone-producing lesions. It may detect several types of pAATLs (which, for convenience, we reference as pAATL types 1–3 in this paper). The pAATLs that we previously reported (Nishimoto et al., 2016a,b) as well as those in Cases 1 and 2 were similar, in that they had subcapsular APCC-like portions and mAPA-like portions (pAATL-type 1). It appears that, when pAATL-type 1 nodules grow larger than 3 mm, they often harbor a *KCNJ5* mutation, which suggests that the *KCNJ5* mutations might be a second hit mutation, rather than a causal mutation of pAATL. This is consistent with two important findings: 1) In depth re-sequencing of the adrenals found that adrenal hyperplasia causing unilateral aldosterone hypersecretion did not harbor the *KCNJ5* mutations (Akerstrom et al., 2012). 2) *KCNJ5* mutations did not increase cell proliferation *in vitro* (Gomez-Sanchez and Gomez-Sanchez, 2012; Oki et al., 2012). Our results also extend the knowledge of the diversity of pAATLs; the lesions in Case 3 (pAATL-type 2) and Case 4 (pAATL-type 3) differed from pAATL-type 1 in their immunohistochemical appearances and somatic mutation characteristics. Further immunohistochemical analyses are needed in order to clearly define pAATL types and develop novel methods that directly detect hormone levels in adrenocortical tissues.

Supplementary Material

Refer to Web version on PubMed Central for supplementary material.

Acknowledgments

We thank Dr. Takeshi Yamazaki at Hiroshima University for providing us with the antibodies for 3βHSD; Mr. Shinya Sasai at Tachikawa Hospital for his technical assistance with immunohistochemistry; as well as funding support from the Japan Society for the Promotion of Science (KAKENHI-Grants to K.N [26893261] and KM [#26461387]), the Suzuken Memorial Foundation (to KN), Yamaguchi Endocrine Research Foundation (to KN), Okinaka Memorial Institute for Medical Research (to KN), Federation of National Public Service Personnel Mutual Aid Associations (to KN), NIH HL27255 (to CEG-S) and Initiative for Rare and Undiagnosed Diseases (IRUD) by AMED (to YK). This study was approved by the Institutional Review Board of Keio University School of Medicine (approval number: 2009–0018), Hiroshima University (#hi [Japanese Katakana letter]-1-8), Yokohama Rosai Hospital (#24-10), and National Hospital Organization Kyoto Medical Center (#12-25).

References

Akehi Y, Kawate H, Murase K, Nagaishi R, Nomiyama T, Nomura M, Takayanagi R, Yanase T. Proposed diagnostic criteria for subclinical Cushing's syndrome associated with adrenal incidentaloma. Endocr J. 2013; 60:903–912. [PubMed: 23574729]

Akerstrom T, Crona J, Delgado Verdugo A, Starker LF, Cupisti K, Willenberg HS, Knoefel WT, Saeger W, Feller A, Ip J, Soon P, Anlauf M, Alesina PF, Schmid KW, Decaussin M, Levillain P, Wangberg B, Peix JL, Robinson B, Zedenius J, Backdahl M, Caramuta S, Iwen KA, Botling J, Stalberg P, Kraimps JL, Dralle H, Hellman P, Sidhu S, Westin G, Lehnert H, Walz MK, Akerstrom G, Carling T, Choi M, Lifton RP, Bjorklund P. Comprehensive re-sequencing of adrenal aldosterone producing lesions reveal three somatic mutations near the KCNJ5 potassium channel selectivity filter. PLoS One. 2012; 7:e41926. [PubMed: 22848660]

Azizan EA, Poulsen H, Tuluc P, Zhou J, Clausen MV, Lieb A, Maniero C, Garg S, Bochukova EG, Zhao W, Shaikh LH, Brighton CA, Teo AE, Davenport AP, Dekkers T, Tops B, Kusters B, Ceral J, Yeo GS, Neogi SG, McFarlane I, Rosenfeld N, Marass F, Hadfield J, Margas W, Chaggar K, Solar M, Deinum J, Dolphin AC, Farooqi IS, Striessnig J, Nissen P, Brown MJ. Somatic mutations in ATP1A1 and CACNA1D underlie a common subtype of adrenal hypertension. Nat Genet. 2013; 45:1055–1060. [PubMed: 23913004]

Beuschlein F, Boulkroun S, Osswald A, Wieland T, Nielsen HN, Lichtenauer UD, Penton D, Schack VR, Amar L, Fischer E, Walther A, Tauber P, Schwarzmayr T, Diener S, Graf E, Allolio B, Samson-Couterie B, Benecke A, Quinkler M, Fallo F, Plouin PF, Mantero F, Meitinger T, Mulatero P, Jeunemaitre X, Warth R, Vilsen B, Zennaro MC, Strom TM, Reincke M. Somatic mutations in ATP1A1 and ATP2B3 lead to aldosterone-producing adenomas and secondary hypertension. Nat Genet. 2013; 45:440–4. 444e1–2. [PubMed: 23416519]

Boulkroun S, Beuschlein F, Rossi GP, Golib-Dzib JF, Fischer E, Amar L, Mulatero P, Samson-Couterie B, Hahner S, Quinkler M, Fallo F, Letizia C, Allolio B, Ceolotto G, Cicala MV, Lang K, Lefebvre H, Lenzini L, Maniero C, Monticone S, Perrocheau M, Pilon C, Plouin PF, Rayes N, Seccia TM, Veglio F, Williams TA, Zinnamosca L, Mantero F, Benecke A, Jeunemaitre X, Reincke M, Zennaro MC. Prevalence, clinical, and molecular correlates of KCNJ5 mutations in primary aldosteronism. Hypertension. 2012; 59:592–598. [PubMed: 22275527]

Choi M, Scholl UI, Yue P, Bjorklund P, Zhao B, Nelson-Williams C, Ji W, Cho Y, Patel A, Men CJ, Lolis E, Wisgerhof MV, Geller DS, Mane S, Hellman P, Westin G, Akerstrom G, Wang W, Carling T, Lifton RP. K+ channel mutations in adrenal aldosterone-producing adenomas and hereditary hypertension. Science. 2011; 331:768–772. [PubMed: 21311022]

Curnow KM, Tusie-Luna MT, Pascoe L, Natarajan R, Gu JL, Nadler JL, White PC. The product of the CYP11B2 gene is required for aldosterone biosynthesis in the human adrenal cortex. Mol Endocrinol. 1991; 5:1513–1522. [PubMed: 1775135]

Dekkers T, Ter Meer M, Lenders JW, Hermus AR, Schultze Kool L, Langenhuijsen JF, Nishimoto K, Ogishima T, Mukai K, Azizan EA, Tops B, Deinum J, Kusters B. Adrenal nodularity and somatic mutations in primary aldosteronism: one node is the culprit? J Clin Endocrinol Metab. 2014; 99:E1341–E1351. [PubMed: 24758183]

Domalik LJ, Chaplin DD, Kirkman MS, Wu RC, Liu WW, Howard TA, Seldin MF, Parker KL. Different isozymes of mouse 11 beta-hydroxylase produce mineralocorticoids and glucocorticoids. Mol Endocrinol. 1991; 5:1853–1861. [PubMed: 1686470]

Enberg U, Volpe C, Hoog A, Wedell A, Farnebo LO, Thoren M, Hamberger B. Postoperative differentiation between unilateral adrenal adenoma and bilateral adrenal hyperplasia in primary aldosteronism by mRNA expression of the gene CYP11B2. Eur J Endocrinol. 2004; 151:73–85. [PubMed: 15248825]

Erdmann B, Gerst H, Bulow H, Lenz D, Bahr V, Bernhardt R. Zone-specific localization of cytochrome P45011B1 in human adrenal tissue by PCR-derived riboprobes. Histochem Cell Biol. 1995; 104:301–307. [PubMed: 8548564]

Funder JW, Carey RM, Fardella C, Gomez-Sanchez CE, Mantero F, Stowasser M, Young WF Jr, Montori VM, Endocrine S. Case detection, diagnosis, and treatment of patients with primary aldosteronism: an endocrine society clinical practice guideline. J Clin Endocrinol Metab. 2008; 93:3266–3281. [PubMed: 18552288]

Gomez-Sanchez CE, Gomez-Sanchez EP. Mutations of the potassium channel KCNJ5 causing aldosterone-producing adenomas: one or two hits? Hypertension. 2012; 59:196–197. [PubMed: 22203746]

Gomez-Sanchez CE, Qi X, Velarde-Miranda C, Plonczynski MW, Parker CR, Rainey W, Satoh F, Maekawa T, Nakamura Y, Sasano H, Gomez-Sanchez EP. Development of monoclonal antibodies against human CYP11B1 and CYP11B2. Mol Cell Endocrinol. 2014; 383:111–117. [PubMed: 24325867]

Imai M, Shimada H, Okada Y, Matsushima-Hibiya Y, Ogishima T, Ishimura Y. Molecular cloning of a cDNA encoding aldosterone synthase cytochrome P-450 in rat adrenal cortex. FEBS Lett. 1990; 263:299–302. [PubMed: 2129527]

Kawamoto T, Mitsuuchi Y, Toda K, Yokoyama Y, Miyahara K, Miura S, Ohnishi T, Ichikawa Y, Nakao K, Imura H, et al. Role of steroid 11 beta-hydroxylase and steroid 18-hydroxylase in the biosynthesis of glucocorticoids and mineralocorticoids in humans. Proc Natl Acad Sci U S A. 1992; 89:1458–1462. [PubMed: 1741400]

Lauber M, Sugano S, Ohnishi T, Okamoto M, Muller J. Aldosterone biosynthesis and cytochrome P-45011 beta: evidence for two different forms of the enzyme in rats. J Steroid Biochem. 1987; 26:693–698. [PubMed: 3613569]

Mitani F, Suzuki H, Hata J, Ogishima T, Shimada H, Ishimura Y. A novel cell layer without corticosteroid-synthesizing enzymes in rat adrenal cortex: histochemical detection and possible physiological role. Endocrinology. 1994; 135:431–438. [PubMed: 8013381]

Mornet E, Dupont J, Vitek A, White PC. Characterization of two genes encoding human steroid 11 beta-hydroxylase (P-450(11) beta). J Biol Chem. 1989; 264:20961–20967. [PubMed: 2592361]

Mukai K, Imai M, Shimada H, Ishimura Y. Isolation and characterization of rat CYP11B genes involved in late steps of mineralo- and glucocorticoid syntheses. J Biol Chem. 1993; 268:9130–9137. [PubMed: 8473352]

Nanba K, Tsuiki M, Sawai K, Mukai K, Nishimoto K, Usui T, Tagami T, Okuno H, Yamamoto T, Shimatsu A, Katabami T, Okumura A, Kawa G, Tanabe A, Naruse M. Histopathological diagnosis of primary aldosteronism using CYP11B2 immunohistochemistry. J Clin Endocrinol Metab. 2013; 98:1567–1574. [PubMed: 23443813]

Nishikawa T, Omura M, Satoh F, Shibata H, Takahashi K, Tamura N, Tanabe A. Task Force Committee on Primary Aldosteronism T.J.E.S. Guidelines for the diagnosis and treatment of primary aldosteronism–the Japan Endocrine Society 2009. Endocr J. 2011; 58:711–721. [PubMed: 21828936]

Nishimoto K, Nakagawa K, Li D, Kosaka T, Oya M, Mikami S, Shibata H, Itoh H, Mitani F, Yamazaki T, Ogishima T, Suematsu M, Mukai K. Adrenocortical zonation in humans under normal and pathological conditions. J Clin Endocrinol Metab. 2010; 95:2296–2305. [PubMed: 20200334]

Nishimoto K, Rigsby CS, Wang T, Mukai K, Gomez-Sanchez CE, Rainey WE, Seki T. Transcriptome analysis reveals differentially expressed transcripts in rat adrenal zona glomerulosa and zona fasciculata. Endocrinology. 2012; 153:1755–1763. [PubMed: 22374966]

Nishimoto K, Rainey WE, Bollag WB, Seki T. Lessons from the gene expression pattern of the rat zona glomerulosa. Mol Cell Endocrinol. 2013; 371:107–113. [PubMed: 23287491]

Nishimoto K, Harris RB, Rainey WE, Seki T. Sodium deficiency regulates rat adrenal zona glomerulosa gene expression. Endocrinology. 2014; 155:1363–1372. [PubMed: 24422541]

Nishimoto K, Tomlins SA, Kuick R, Cani AK, Giordano TJ, Hovelson DH, Liu CJ, Sanjanwala AR, Edwards MA, Gomez-Sanchez CE, Nanba K, Rainey WE. Aldosterone-stimulating somatic gene mutations are common in normal adrenal glands. Proc Natl Acad Sci U S A. 2015; 112:E4591–E4599. [PubMed: 26240369]

Nishimoto K, Seki T, Hayashi Y, Mikami S, Al-Eyd G, Nakagawa K, Morita S, Kosaka T, Oya M, Mitani F, Suematsu M, Kabe Y, Mukai K. Human adrenocortical remodeling leading to aldosterone-producing cell cluster generation. Int J Endocrinol. 2016a; 2016:7834356. [PubMed: 27721827]

Nishimoto K, Seki T, Kurihara I, Yokota K, Omura M, Nishikawa T, Shibata H, Kosaka T, Oya M, Suematsu M, Mukai K. Case report: nodule development from subcapsular aldosterone-producing

cell clusters causes hyperaldosteronism. J Clin Endocrinol Metab. 2016b; 101:6–9. [PubMed: 26580238]

Ogishima T, Mitani F, Ishimura Y. Isolation of aldosterone synthase cytochrome P-450 from zona glomerulosa mitochondria of rat adrenal cortex. J Biol Chem. 1989; 264:10935–10938. [PubMed: 2738055]

Ogishima T, Shibata H, Shimada H, Mitani F, Suzuki H, Saruta T, Ishimura Y. Aldosterone synthase cytochrome P-450 expressed in the adrenals of patients with primary aldosteronism. J Biol Chem. 1991; 266:10731–10734. [PubMed: 2040591]

Ogishima T, Suzuki H, Hata J, Mitani F, Ishimura Y. Zone-specific expression of aldosterone synthase cytochrome P-450 and cytochrome P-45011 beta in rat adrenal cortex: histochemical basis for the functional zonation. Endocrinology. 1992; 130:2971–2977. [PubMed: 1572304]

Ohnishi T, Wada A, Lauber M, Yamano T, Okamoto M. Aldosterone biosynthesis in mitochondria of isolated zones of adrenal cortex. J Steroid Biochem. 1988; 31:73–81. [PubMed: 3398531]

Oki K, Plonczynski MW, Luis Lam M, Gomez-Sanchez EP, Gomez-Sanchez CE. Potassium channel mutant KCNJ5 T158A expression in HAC-15 cells increases aldosterone synthesis. Endocrinology. 2012; 153:1774–1782. [PubMed: 22315453]

Omura M, Sasano H, Fujiwara T, Yamaguchi K, Nishikawa T. Unique cases of unilateral hyperaldosteronemia due to multiple adrenocortical micronodules, which can only be detected by selective adrenal venous sampling. Metabolism. 2002; 51:350–355. [PubMed: 11887172]

Pascoe L, Jeunemaitre X, Lebrethon MC, Curnow KM, Gomez-Sanchez CE, Gasc JM, Saez JM, Corvol P. Glucocorticoid-suppressible hyperaldosteronism and adrenal tumors occurring in a single French pedigree. J Clin Investig. 1995; 96:2236–2246. [PubMed: 7593610]

Sakuma I, Saito J, Matsuzawa Y, Omura M, Matsui S, Nishimoto K, Mukai K, Nishikawa T. Multiple sampling from the central veins with their tributaries can detect bilateral hyperaldosteronism with a cortisol-producing adenoma in a hypertensive patient. J Steroids Horm Sci. 2014:5.

Sasano H. Localization of steroidogenic enzymes in adrenal cortex and its disorders. Endocr J. 1994; 41:471–482. [PubMed: 7889106]

Scholl UI, Goh G, Stolting G, de Oliveira RC, Choi M, Overton JD, Fonseca AL, Korah R, Starker LF, Kunstman JW, Prasad ML, Hartung EA, Mauras N, Benson MR, Brady T, Shapiro JR, Loring E, Nelson-Williams C, Libutti SK, Mane S, Hellman P, Westin G, Akerstrom G, Bjorklund P, Carling T, Fahlke C, Hidalgo P, Lifton RP. Somatic and germline CACNA1D calcium channel mutations in aldosterone-producing adenomas and primary aldosteronism. Nat Genet. 2013; 45:1050–1054. [PubMed: 23913001]

Shigematsu K, Kawai K, Irie J, Sakai H, Nakashima O, Iguchi A, Shimamatsu J, Shimamatsu K, Kusaba Y, Takahara O. Analysis of unilateral adrenal hyperplasia with primary aldosteronism from the aspect of messenger ribonucleic acid expression for steroidogenic enzymes: a comparative study with adrenal cortices adhering to aldosterone-producing adenoma. Endocrinology. 2006; 147:999–1006. [PubMed: 16282357]

Tamura A, Nishimoto K, Seki T, Matsuzawa Y, Saito J, Omura M, Gomez-Sanchez CE, Makita K, Matsui S, Moriya N, Inoue A, Nagata M, Sasano H, Nakamura Y, Yamazaki Y, Kabe Y, Mukai K, Kosaka T, Oya M, Suematsu S, Nishikawa T. Somatic KCNJ5 mutation occurring early in adrenal development may cause a novel form of juvenile primary aldosteronism. Mol Cell Endocrinol. 2016

Uchida T, Nishimoto K, Fukumura Y, Asahina M, Goto H, Kawano Y, Shimizu F, Tsujimura A, Seki T, Mukai K, Kabe Y, Suematsu M, Gomez-Sanchez CE, Yao T, Horie S, Watada H. Disorganized steroidogenesis in adrenocortical carcinoma, a case study. Endocr Pathol. 2016

Wotus C, Levay-Young BK, Rogers LM, Gomez-Sanchez CE, Engeland WC. Development of adrenal zonation in fetal rats defined by expression of aldosterone synthase and 11beta-hydroxylase. Endocrinology. 1998; 139:4397–4403. [PubMed: 9751524]

Appendix A. Supplementary data

Supplementary data related to this article can be found at http://dx.doi.org/10.1016/j.mce.2016.10.014.

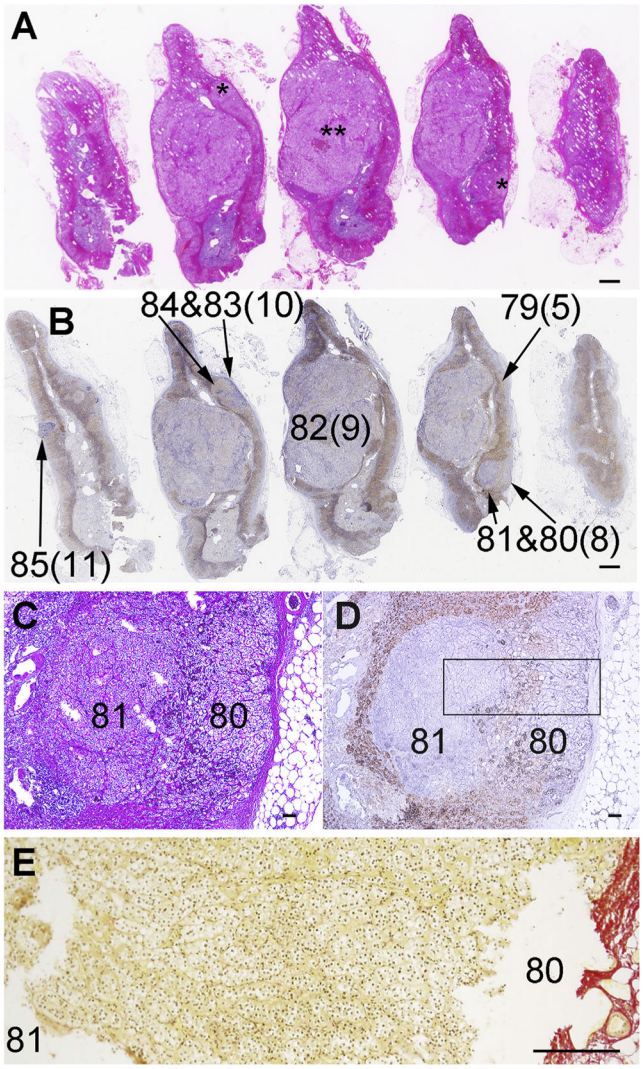

Fig. 1.

Histology of Case 1 adrenal. A: Hematoxylin and eosin staining. *: small nodules. **: a large nodule. B: Double-immunostaining for CYP11B2 (blue; in-house polyclonal antibody and 5-bromo-4-chloro-3-indolyl-phosphate with nitro blue tetrazolium) and CYP11B1 (brown; in-house polyclonal antibody and 3,3′-diaminobenzidine) as previously reported (Nishimoto et al., 2010). Numbers without parenthesis indicate areas from which DNAs/RNAs were prepared (DNA/RNA numbers in Table 2 and Supplemental Table 1). Numbers in parenthesis indicate Control# or pAATL# for the corresponding DNA/RNA numbers. C and D: H&E and IHC, respectively: Enlarged images of a representative pAATL with subcapsular APCC-like and inner microAPA-like lesions (pAATL#3) (Table 2), which used for preparation of DNA/RNA 80 and 81, respectively. E: Enlarged image of Sirius Red staining on a serial section used for microdissection. The image area corresponds to the boxed area in Fig. 1D. Scale bars in panels A–B, C–D, and E indicate 1 mm, 100 μm, and 200 μm, respectively.

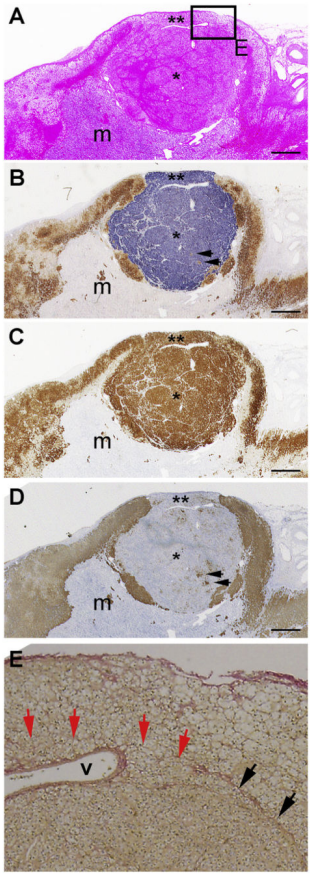

Fig. 2.

Histology of Case 2 adrenal. Serial sections of a nodule (*) and the adjacent adrenal gland; m: adrenal medulla, ** APCC-like portion of pAATL, Arrows in panels B and D indicate presumed cortisol producing cells expressing CYP11B1 and CYP17. A: Hematoxylin and eosin staining. B: Double-immunostaining for CYP11B2 (blue) and CYP11B1 (brown), monoclonal antibodies from Dr. Gomez-Sanchez (Gomez-Sanchez et al., 2014); m: medulla C: Immunohistochemistry for 3βHSD, polyclonal antibody from Dr. Yamazaki with hematoxylin nuclear staining (Nishimoto et al., 2010). D: Immunohistochemistry for CYP17, monoclonal antibody from Dr. Gomez-Sanchez (Uchida et al., 2016) with hematoxylin nuclear staining. E: Enlarged image of Sirius Red staining on a serial section. The image area corresponds to the boxed area in Fig. 2A. Black arrows indicate fibrous border between normal adrenal gland and mAPA-like lesion. Red arrows indicate possible border between APCC-like and mAPA-like regions, where no obvious fibrous border was observed. “v”: vessel. Scale bars indicate 1 mm in panels A–D.

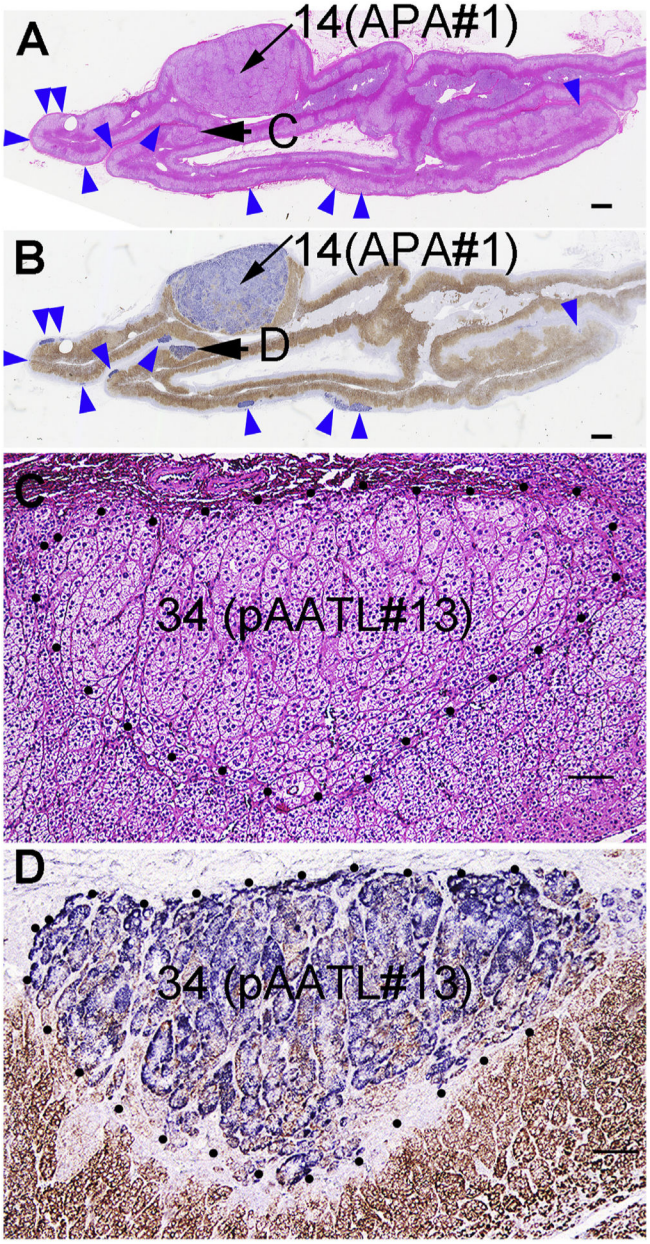

Fig. 3.

Histology of Case 3 adrenal. (presented at the Adrenal Cortex 2016 meeting in Boston). A: Hematoxylin and eosin staining. B: double-immunostaining for CYP11B2 (blue) and CYP11B1 (brown) (monoclonal antibodies from Dr. Gomez-Sanchez) of whole adrenal sections through the APA #1. A & B: Blue arrowheads: APCCs. C and D: Enlarged images of the pAATL indicated by arrows in panels A & B (pAATL #13, Table 2, Supplementary Table 1). Numbers indicate corresponding DNA/RNA numbers. Scale bars in panels A–B and C–D indicate 1 mm and 100 μm, respectively.

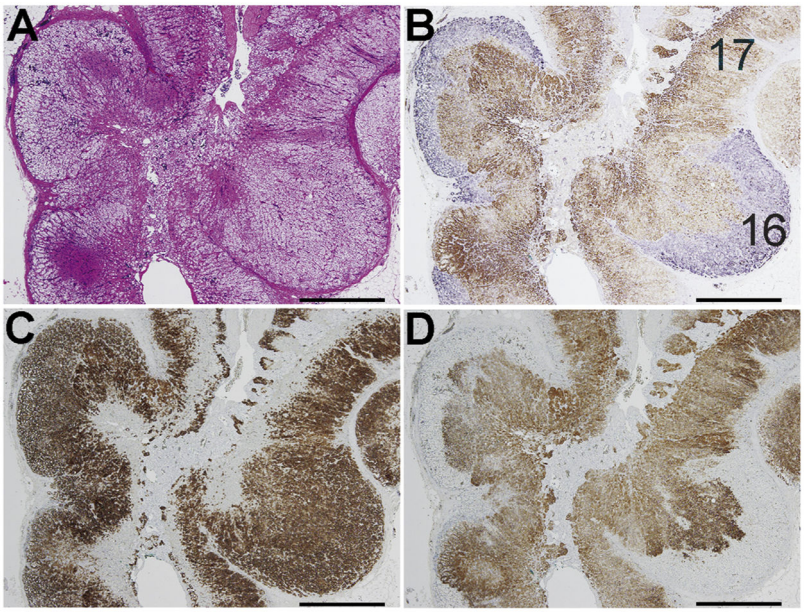

Fig. 4.

Histology of Case 4 adrenal. A: Hematoxylin and eosin staining. B: Double-immunostaining for CYP11B2 (blue, polyclonal in-house antibody) and CYP11B1 (brown, polyclonal in-house antibody). C & D: single-immunostaining with hematoxylin nuclear staining for 3βHSD and CYP17 (both antibodies from Dr. Yamazaki). Numbers in panel B indicate corresponding DNA/RNA numbers (16: pAATL #14, 17: control #7; Table 2; Supplementary Table 1).

Table 1

Patient characteristics and hormonal test data.

Case #	age (year)	sex	hight	weight	BMI (kg/m2)	screening test for PA			confirmatory tests for PA							adrenal venous sampling data										
						PAC	PRA	ARR	SIT (PAC after infusion)	captopril challenge test					FUT (PRA after loading)	right adrenal vein data			left adrenal vein data			peripheral vein data			lateralization data	
										PAC pre	PAC post	PRA post	ARR post	% decrease of PAC		PAC	PCC	ACR	PAC	PCC	ACR	PAC	PCC	ACR	LR	CR
normal range/cut off					<25	39–159	0.3–2.9	<200	<50*/<60**				<200*	>30**	<1*										>4*/>2.6**	<1
1	64	M	167.8	61.7	21.9	214	0.4	535.0	NA	132	97	0.2	485	26.5	0.9	6514	529.8	12.3	32,180	511	63.0	199	17.4	11.4	5.12	1.08
2	61	M	169.2	56.0	19.6	198	0.3	660.0	NA	158	94.8	0.5	189.6	40.0	1.4	9100	1115	8.2	72,800	1188	61.3	225	19.3	11.6	7.51	0.70
3	35	F	152.4	49.8	21.4	229	0.4	572.5	336	310	283	1	283	8.7	0.8	19,800	822	24.1	53,300	446	119.5	700	24.3	28.8	4.96	0.84
4	37	M	162.0	62.2	23.7	233	0.7	332.9	80	130	125	0.4	312.5	3.8	1.3	7420	1160	6.4	39,500	988	40.0	320	27.5	11.6	6.25	0.55

BMI: body mass index (normal range: <25), M: male, F: female, PAC: plasma aldosterone concentration (pg/mL), PRA: plasma renin activity (ng/ml/h),

*criteria in US guideline of PA (Funder et al., 2008),

**criteria in Japanese Guideline of PA (Nishikawa et al., 2011),

FUT: furosemide upright test, PCC: plasma cortisol concentration, ACR: aldosterone cortisol ratio (PAC/PCC), LR: lateralized ratio, CR: contralateral ratio, NA: not available, PA: primary aldosteronism, SIT: saline infusion test.

Table 2

Sample information and NGS results using these samples.

Case	sample description		DNA/RNA#	CYP11B2 mRNA level (S.E.M. range)	high confidence somatic non-synonymous variants				
					gene	location	amino acid change	variant allele frequency (%, FAO/FDP)	frequency in matched controls
1	Control 5		79	1.0(0.9–1.1)	(−)				
	pAATL 8	outer	80	19,53,324.2(17,39,329.1–21,93,647.8)	(−)				
		inner	81	38,86,392.0(35,55,559.1–42,48,007.8)	(−)				
	pAATL 9		82	10,79,925.2(9,45,969.3–12,32,850.2)	*KCNJ5*	chr11:128781619	p.Gly151Arg	28.8	0.1
	pAATL 10	outer	83	35,57,666.9(32,53,666.1–38,90,071.5)	*ATP1A1*	chr1:116930041	p.Trp105Ter	93.8	0.0
					CACNA1D	chr3:53806922	p.Met1389Ile	42.4	0.0
					ATP2B3	chrX:152814205	p.Val411Ile	69.8	0.0
		inner	84	1.0(9,71,447.9–15,89,589.6)	(−)				
	pAATL 11		85	6,24,568.4(5,79,318.4–6,73,352.8)	*ATP1A1*	chr1:116930004	p.Cys93Tyr	98.8	0.0
					ATP1A1	chr1:116930032	p.Met102Ile	100.0	0.1
					ATP1A1	chr1:116930037	p.Leu104Pro	20.7	0.2
					ATP1A1	chr1:116930045	p.Gly107Arg	98.9	0.1
					ATP1A1	chr1:116930084	p.Ala120Thr	100.0	0.1
					CACNA1D	chr3:53707815	p.Leu398Phe	27.8	0.1
					CACNA1D	chr3:53707816	p.Leu398Pro	19.5	0.3
					CACNA1D	chr3:53764549	p.Glu788Lys	57.9	0.1
					CACNA1D	chr3:53783422	p.Val1168Met 22.1		0.0
2	pAATL 12		NA						
3	Control 6		15	1.0(0.6–1.5)	(−)				
	APA 2		13	16,03,174(12,11,822–21,20,912)	*KCNJ5*	chr11:128781671	p.Leu168Arg	33.7	0.0
	APA 1		14	1,78,26,251(1,30,86,736–2,42,82,236)	*KCNJ5*	chr11:128781671	p.Leu168Arg	34.9	0.0
	pAATL 13		34	20,86,278(15,31,683–28,41,682)	*ATP1A1*	chr1:116932294	p.Ala330Thr	15.0	0.1
					KCNJ5	chr11:128781631	p.Arg155Ter	32.5	0.0
					KCNJ5	chr11:128781664	p.Ile166Val	25.2	0
4	Control 7		17	1.0(0.4–2.4)	(−)				
	pAATL 14		16	6,56,13,984.6(5,43,16,143.1–7,92,61,794.6)	(−)				

Case	sample description	DNA/RNA#	CYP11B2 mRNA level (S.E.M. range)	high confidence somatic non-synonymous variants				
				gene	location	amino acid change	variant allele frequency (%, FAO/FDP)	frequency in matched controls
	pAATL 15	18	1,99,012.6(98,179.5–4,03,403.9)	(−)				

DNA and RNA were isolated from the FFPE tissues of cases 1, 3, and 4. RNA was used in CYP11B2-qPCR for the confirmation of sample collection. CYP11B2 mRNA levels were shown by fold changes from corresponding control samples (control #5 for pAATLs #8–#11, control #6 for APA 1–2 and pAATL #13, as well as control #7 for pAATL #14–15). Libraries were prepared from DNA and were used for NGS, the results of which are shown in Table 1 and Supplemental Tables 1–2. The columns list the Case #, Sample Description, Assigned DNA/RNA number, CYP11B2-mRNA level, information of High-Confidence Somatic Nonsynonymous Variants including gene symbol (gene), chromosome location in a human reference genome (i.e., hg19) (location), amino acid changes, and percentage of variant allele frequency. The variant allele frequencies in the matched control tissues (controls #5–7) are shown for comparison. Detailed information on NGS is available in Supplemental Tables 1–2. NA: not available.